JOURNAL OF GEOPHYSICAL RESEARCH, VOL. 93, NO. A3, PAGES 1922–1932, MARCH 1, 1988

Comparison of Simultaneous Chatanika and Millstone Hill Temperature Measurements With Ionospheric Model Predictions

C. E. RASMUSSEN, J. J. SOJKA, AND R. W. SCHUNK

Center for Atmospheric and Space Sciences, Utah State University, Logan

V. B. WICKWAR AND O. DE LA BEAUJARDIERE

SRI International, Menlo Park, California

J. FOSTER AND J. HOLT

MIT Haystack Observatory, Westford, Massachusetts

As part of the MITHRAS program, the Chatanika and Millstone Hill incoherent scatter radars made coordinated observations of the polar ionosphere on June 27 and 28, 1981. The temperature data obtained during these days were compared with predictions made by a high-latitude ionospheric model. The comparison of the temperature measurements and the results of the ionospheric model depend on the assumptions made both in reducing the data and on the inputs that are needed by the model. The deduction of electron temperature from radar measurements depends upon a knowledge of the mean ion mass as a function of altitude. The model requires a knowledge of the heat flux at the upper boundary and the volume heating rate. The results of the model were compared with measurements for a variety of combinations of the required inputs. It was found that the best fits resulted with a heat flux of from 0 to -0.7×10^{10} eV cm^{-2} s^{-1} at the upper boundary and a relatively high volume heating rate. These results also required that the model predictions for the average ion mass be used in the reduction of the radar data. However, other combinations of assumptions also produced good fits. A systematic temperature difference of between 200 and 300 K was found between the Chatanika and Millstone Hill measurements of electron temperature at high altitudes.

1. INTRODUCTION

Between May 1981 and June 1982, an intensive campaign of 33 coordinated observations was carried out using three incoherent scatter radars: the Chatanika (Alaska); Millstone Hill (Massachusetts); and European Incoherent Scatter (EISCAT) (Scandinavia) facilities [*de la Beaujardiere et al.*, 1984]. At times, the Scandinavian Twin Auroral Radar Experiment (STARE) was able to provide additional coverage. This experimental campaign has become known as the Magnetosphere-Ionosphere-Thermosphere Radar Studies (MITHRAS) program, and the data base obtained from the campaign provides an excellent opportunity for a comparison of our ionospheric model with observations.

This comprehensive model of the convecting high-latitude ionosphere has been developed in order to determine the extent to which various chemical and transport processes affect the ion and electron temperature, the ion composition, and the electron density at *F* region altitudes [cf. *Schunk and Raitt*, 1980; *Sojka et al.*, 1981*a*; *Schunk and Sojka*, 1982; *Schunk et al.*, 1986]. Our numerical model produces time-dependent, three-dimensional distributions for the ion and electron temperatures and the ion (NO^+, N_2^+, O_2^+, N^+, O^+, He^+) and electron densities. The model takes account of field-aligned diffusion, cross-field electrodynamic drifts, thermospheric winds, energy-dependent chemical reactions, neutral composition changes, ion production due to solar EUV radiation and auroral precipitation, ion thermal conduction, ion diffusion-thermal heat flow, and local heating and cooling processes. Our model also takes account of the offset between the geomagnetic and geographic poles [*Sojka et al.*, 1979].

Sojka et al. [1983] have made an initial comparison of the model with a portion of the MITHRAS data which covered a 24-hour period beginning on October 13, 1979. This was then followed by a comprehensive comparison of the ionospheric model with electron density measurements made by the Chatanika and Millstone Hill radars on June 27 and 28, 1981 [*Rasmussen et al.*, 1986]. The results of the later study showed that the model predicts quite well the electron density features of the high-latitude ionosphere during summer conditions. In that study [*Rasmussen et al.*, 1986], electron temperatures were not computed rigorously, but were inputs to the model and were obtained from radar data. Recently, the high-latitude model has been improved by including the electron energy equation so that the electron temperature is self-consistently calculated [*Schunk et al.*, 1986]. This allows us, in the present work, to extend the study of *Rasmussen et al.* [1986] to include a comparison of the electron and ion temperature measurements with the improved ionospheric model. This is the first detailed comparison of electron temperatures predicted by our ionospheric model with measurements.

In the *Rasmussen et al.* [1986] study the electron density measurements were compared over the full latitudinal range of the radar measurements. This made it possible to compare such density features as the mid-latitude trough with model predictions. We found that the electron temperature is more sensitive to the input parameters than is the electron density. In particular, the electron temperature is sensitive to the amount of heat flux coming from the magnetosphere and to the volume heating rate due to both photoelectrons and precipitating auroral electrons. Because of this sensitivity, we concentrated on altitude comparisons rather than latitudinal coverage. This allows for a

Paper number 7A9186.
0148-0227/88/007A-9186$05.00

better understanding of the effects of the heat flux and volume heating rate on electron temperatures.

Another difference is noted from the original study. In the *Rasmussen et al.* [1986] study, the inputs to the ionospheric model were very carefully selected from various measurements made by the three radars and the NOAA 6 satellite on the two days studied. Owing to a lack of precise measurements of parameters that affect the electron temperature, we could not determine all of the input parameters as was the case in the previous study. Rather, the heat flux and the volume heating rate were varied over a range of likely values, and the results compared with measurements. All other model inputs were the same as in the *Rasmussen et al.* [1986] study.

The paper proceeds by first providing a brief description of the ionospheric model along with a description of the manner in which the radar measurements were made. Particular attention is paid to uncertainties in data reduction due to an imprecise knowledge of the mean ion mass. Then, the model results are compared with the Millstone Hill and Chatanika temperature measurements, and finally, we end with a discussion of the conclusions that can be drawn from this study.

2. RADAR-MODEL OVERVIEW

2.1. *Ionospheric Model*

The ionospheric model was initially developed as a mid-latitude, multi-ion (NO^+, O_2^+, N_2^+, and O^+) model by *Schunk and Walker* [1973]. The time-dependent ion continuity and momentum equations were solved as a function of altitude for a corotating plasma flux tube including diurnal variations and all relevant E and F region processes. This model was extended to include high-latitude effects due to convection electric fields and particle precipitation by *Schunk et al.* [1975, 1976]. A simplified ion energy equation was also added, which was based on the assumption that local heating and cooling processes dominate (valid below 500 km). Flux tubes of plasma were followed as they moved in response to convection electric fields. A further extension of the model to include the minor ions N^+ and He^+, an updated photochemical scheme, and the mass spectrometer-incoherent scatter (MSIS) atmospheric model is described by *Schunk and Raitt* [1980].

The addition of plasma convection and particle precipitation models is described by *Sojka et al.* [1981*a*, *b*]. More recently, the ionospheric model has been extended by *Schunk and Sojka* [1982] to include ion thermal conduction and diffusion-thermal heat flow, so that the ion temperature is now rigorously calculated at all altitudes between 120 and 1000 km. The adopted ion energy equation and conductivities are those given by *Conrad and Schunk* [1979]. Also, the electron energy equation has been included recently by *Schunk et al.* [1986], and consequently, the electron temperature is now rigorously calculated at all altitudes. The electron energy equation and the heating and cooling rates were taken from *Schunk and Nagy* [1978], and the conductivities were taken from *Schunk and Walker* [1970]. The incorporation of the *Sterling et al.* [1969] equatorial ionospheric model and the various improvements to this model are described by *Sojka and Schunk* [1985].

2.2. *Radar-Deduced Temperatures*

Chatanika. The data for June 27 to 28, 1981, from Chatanika were acquired in the MITHRAS 1 mode [*de la Beaujardiere et al.*, 1984]. Briefly, this mode was designed to provide an extended set of geophysical parameters over a wide range of invariant latitude with about a 30-min time resolution. The wide range was obtained by using F region measurements—the higher the altitude, the wider the range. As a consequence, the experimental setup was optimized for F region parameters. Nonetheless, some E region parameters were obtained over a small range of invariant latitude.

The spectral observations and the determination of electron densities and temperatures have been described by *Baron* [1977] and *Kofman and Wickwar* [1980]. These parameters were derived from 11-position measurements at six invariant latitudes: five pairs straddling the magnetic meridian plane at 29° geographic azimuth and one position parallel to the magnetic field [*Foster et al.*, 1981]. Therefore, measurements from the same altitude in a pair of positions were at the same invariant latitude. It also follows that the lowest-altitude measurements were closest to the radar and had the smallest east-west separation. In each position, eight complete spectral measurements (for the derivation of all parameters) were made between 120 and 480 km altitude, and power measurements (for N_e derivation) were made every 9 km in range throughout the E and F regions. After every five of these sets of measurements, the mode changed for 12.5 min. During that time the antenna performed a continuous elevation scan in the magnetic meridian plane from 25° above the southern horizon to 25° above the northern horizon. The same set of spectral and power measurements was made during these elevation scans.

A 320-μs pulse length was used for all the measurements, which means that the ionospheric parameters are convolved over 48 km along the radar line of sight (actually somewhat more for the spectral measurements). This convolution has little effect in the topside F region, where the scale length for variation is usually much bigger than this value. In the E and the bottomside F regions, it distorts the density profile, but has little effect on height-integrated quantities.

Millstone Hill. The F region electron density and the ion and electron temperatures were derived from measured incoherent scatter spectra. The Millstone Hill measurements were made with the fully steerable 46-m antenna. This antenna was operated in a "scanning" mode, in which it was moved slowly and continuously in azimuth, while the incoherent scatter returns were integrated in the computer and recorded on magnetic tape at regular angle increments. The data acquisition mode utilized on June 27–28, 1981, differed somewhat from the usual MITHRAS 1 procedure [*de la Beaujardiere et al.*, 1984]. Because of antenna upgrading work in progress, the antenna was scanned back and forth in a "windshield wiper" motion. Normally, the antenna is returned rapidly to its start position after the completion of each scan, so that all scans are in the same direction. The main effect on the June 1981 data is a somewhat uneven sampling pattern when the data are displayed versus time and latitude.

During the scans the elevation of the antenna was held constant at 4°. The azimuth was scanned between 177.5° and 267.5° at a fixed scan rate of 10 deg/min. The integration time was 30 s. Single 2000-μs pulses were employed, with 19 range gates spaced 150 km apart. The invariant latitude coverage of each scan was 46°–64° at 160 km, 42°–69° at 325 km, and 39°–72° at 480 km. The local time coverage of the scans was 2.5 hours at 160 km, 3.7 hours at 325 km, and 4.5 hours at 480 km.

2.3. *Effect of the Atomic/Molecular Transition Height on Radar Data*

The mean ion mass plays an important role in the reduction of electron and ion temperature measurements from raw radar

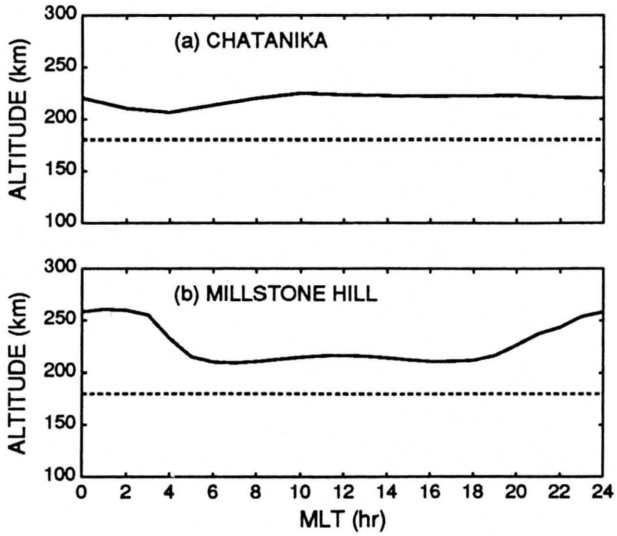

Fig. 1. Diurnal variation of the atomic/molecular ion transition height. (*a*) The solid line is the height predicted by the ionospheric model at 65° dipole latitude, and the dashed line is the height normally assumed in the reduction of Chatanika radar data. (*b*) The solid line is the height predicted by the ionospheric model at 55° dipole latitude, and the dashed line is the height normally assumed in the reduction of Millstone Hill radar data.

data. Since the mean ion mass is not measured by the radars, a model or estimate of the ion mass as a function of height must be made before temperatures can be obtained from radar data. The height at which O^+ becomes the dominant ion (the transition height) is an important indicator of the ion mass profile.

Typically, an estimate of 180 km for the transition height is used to reduce the radar data. However, the transition height obtained from our ionospheric model can vary appreciably from 180 km. This is shown in Figure 1, where the transition height is plotted as a function of MLT for the model and compared to that used in the reduction of the radar data. Figure 1*a* corresponds to ionospheric conditions at a longitude near Chatanika and at 65° dipole latitude, while Figure 1*b* corresponds to conditions at a longitude of Millstone Hill, near 55° dipole latitude. It can be seen that the transition height predicted by our ionospheric model is much higher than 180 km, especially at night.

Recently, a technique has been developed whereby information on the ion composition can be obtained directly from incoherent scatter spectra [*Lathuillere et al.*, 1983]. When the technique was used at the EISCAT facility to study ion composition changes in the auroral ionosphere [*Lathuillere and Brekke*, 1985], large variations in the atomic/molecular ion transition height were observed on a daily basis. The transition height variations were related to changes in solar zenith angle, Joule heating, particle precipitation, and electric fields. These measurements therefore support the previous model predictions of a large variability in the atomic/molecular ion transition height at high latitudes [*Schunk et al.*, 1975, 1976; *Schunk and Raitt*, 1980; *Sojka et al.*, 1981*b*].

The effect that the large difference in the transition height (Figure 1) has upon the temperature measurements is shown in Figure 2, where Chatanika temperature data are plotted assuming a transition height of 180 km (dashed line) and 225 km (solid line). There is a relatively large difference between the two sets of points. Near 210 km, this difference is as large as 600°, while at the top and bottom portions of the curves, there is no difference because the same mass ratio was used in the data reduction for this portion of the curve. It is only near the ion transition height where the assumed ion mass becomes critical. At high altitudes it is unlikely that molecular ions are preponderant for long periods of time and, therefore, one can be confident of the electron temperature measurements above 300 km. Throughout the rest of this paper, we plot only temperature data that have been corrected to take into account the transition heights obtained from our ionospheric model.

3. Model-Data Comparisons

Two major heat sources for the ionosphere are solar radiation and auroral precipitation. Since we are dealing with measurements from Millstone Hill at 55° dipole latitude and from Chatanika at 65°, we plot the solar zenith angle for these two locations as a function of MLT in Figure 3*a*. Note that Millstone Hill (dashed line) moves in and out of sunlight during the course of the day, while Chatanika (solid line) is almost always at least partially sunlit, this being a summer study. In Figure 3*b*, the diurnal variation in the auroral energy flux assumed for this study is plotted for the Chatanika location at 65° (see *Rasmussen et al.*, [1986] for more information). Chatanika is located in a region of strong auroral precipitation in the early morning, while the 55° region of the Millstone Hill measurements receives no auroral precipitation. The volume heating rate of thermal electrons due to photoelectrons is also an important input to the ionospheric model. This heating rate is shown in Figure 3*c* for three different solar zenith angles.

Since auroral precipitation adds additional complications, we first consider measurements made near local noon where auroral precipitation for both radars is insignificant. Since the background density of the ionosphere is an important parameter in modeling the electron temperature, care needs to be taken to assure that the ionospheric model is predicting reliable densities before a temperature comparison can be made. Figure 4 shows a comparison of the electron density profile predicted by the model versus measurements made at Millstone Hill at 1200 MLT (and at 55°). The relatively close agreement between the model densities and the measurements provides a basis on

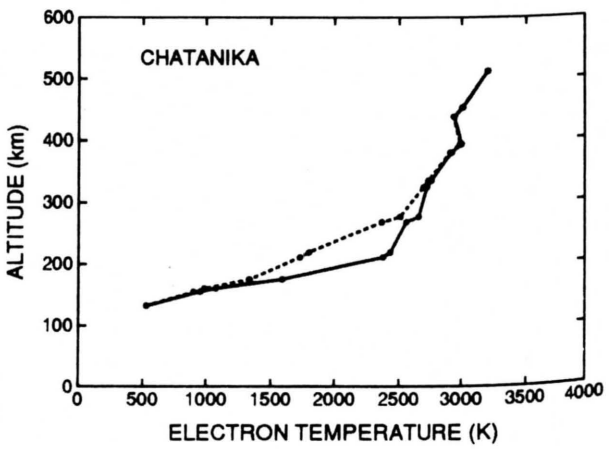

Fig. 2. Effect of the transition height on electron temperature measurements at 1200 MLT. The dashed line connects electron temperature measurements made by the Chatanika radar, assuming the original transition height, and the solid line connects measurements corrected for the transition height predicted by our model.

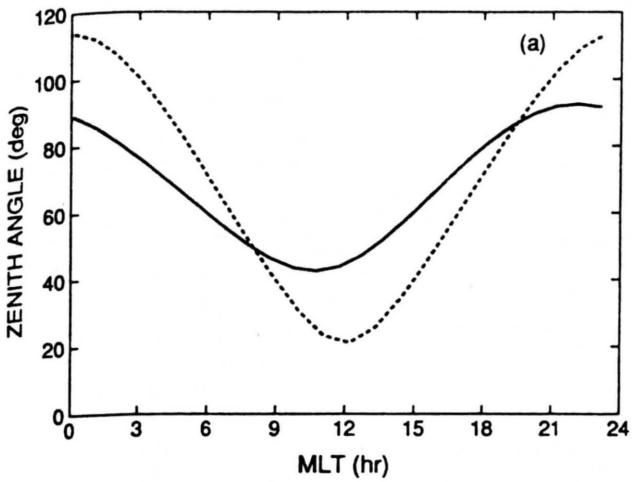

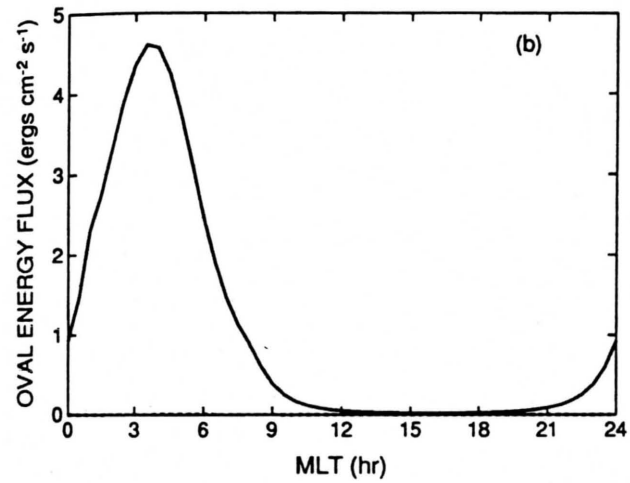

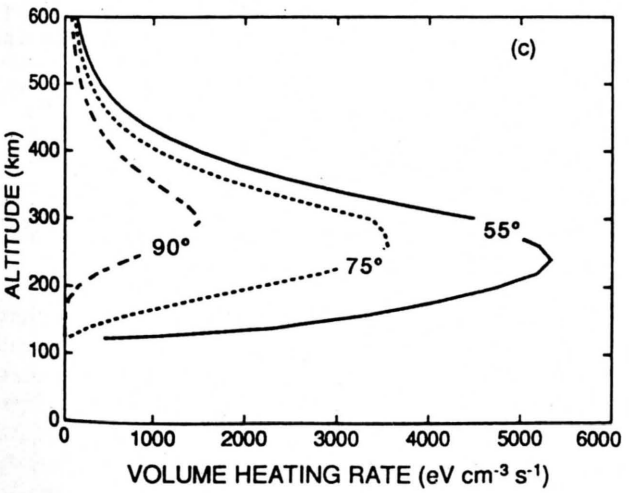

Fig. 3. (*a*) Diurnal variation of the solar zenith angle. (*b*) Diurnal variation of the auroral energy flux. The solid line corresponds to a magnetic dipole latitude of 65° and the dashed line corresponds to a magnetic dipole latitude of 55°. There is no auroral precipitation at 55° dipole latitude. (*c*) The volume heating rate for electrons at three different solar zenith angles.

which to make a comparison between the modeled and measured electron temperatures.

In Figure 5 the electron temperature comparison is made. The solid line represents the model assuming zero heat flux at the upper boundary and a standard volume heating rate (standard referring to the curves in Figure 3*c*). The data show much higher temperatures than are modeled. The short-dashed curve represents a higher heat flux of -2×10^{10} eV cm^{-2} s^{-1}. Although a higher heat flux increases the temperature at high altitudes, this results in an increased temperature gradient, which does not seem to be warranted. An alternative way to increase the temperature is to increase the volume heating rate, as is shown by the long-dashed curve in Figure 5, where a factor of 2.6 increase (above that shown in Figure 3*c*) in the volume heating rate is assumed along with a heat flux of -0.7×10^{10} eV cm^{-2} s^{-1} at the upper boundary. This latter curve most closely fits the data.

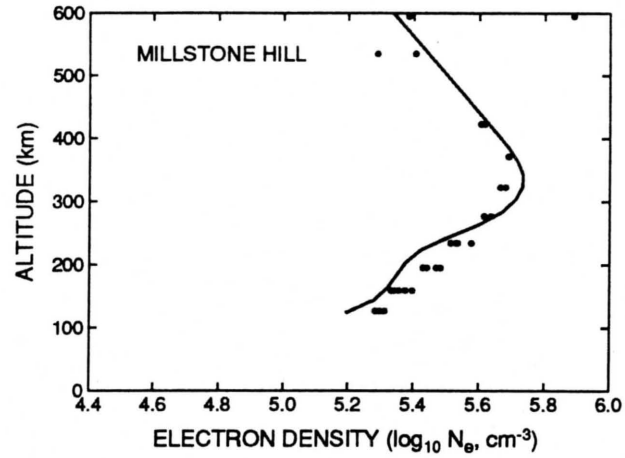

Fig. 4. Comparison of electron density measurements at 1200 MLT with model predictions. Millstone Hill measurements at 55° (± 1°) dipole latitude are plotted as solid circles, and the solid line represents the corresponding ionospheric model results.

Having introduced the dependence on the volume heating rate and the heat flux at the upper boundary, we examine the sensitivity of the electron temperature to these parameters in

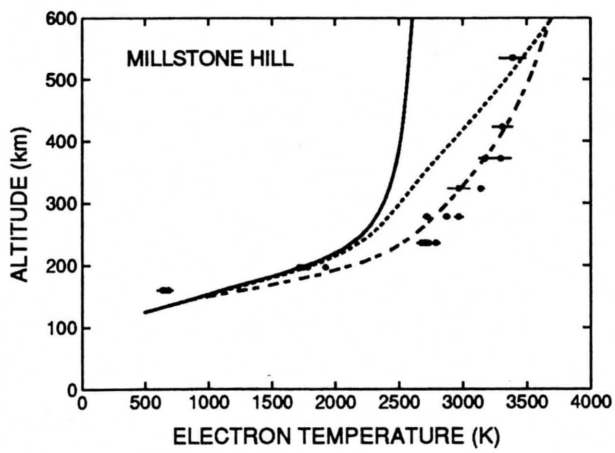

Fig. 5. Comparison of electron temperature measurements with model predictions. Millstone Hill measurements at 55° (± 1°) dipole latitude are plotted as solid circles, and the curves represent the corresponding ionospheric model results. The solid line represents no heat flux and a standard volume heating rate. The short-dashed line represents a heat flux of -2×10^{10} eV cm^{-2} s^{-1} and a standard volume heating rate. The long-dashed line represents a heat flux of -0.7×10^{10} eV cm^{-2} s^{-1} and a factor of 2.6 increase in the volume heating rate.

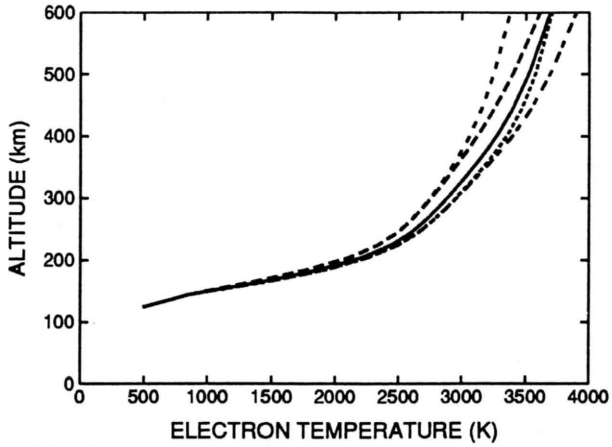

Fig. 6. A plot showing the sensitivity of the model to the heat flux at the upper boundary and the volume heating rate at 1200 MLT and 55° (± 1°) dipole latitude. The solid line represents a volume heating rate of 2.6 times standard and a heat flux of -0.7×10^{10} eV cm^{-2} s^{-1} at the upper boundary. The lower temperature curves correspond to a heating rate of 2.0 times standard, and the higher temperature curves correspond to 3.0 times standard. The lower of each of the two sets of curves represents a heat flux of -0.4×10^{10} eV cm^{-2} s^{-1}, and the upper of each of the two sets of curves represents a heat flux of -1×10^{10} eV cm^{-2} s^{-1}.

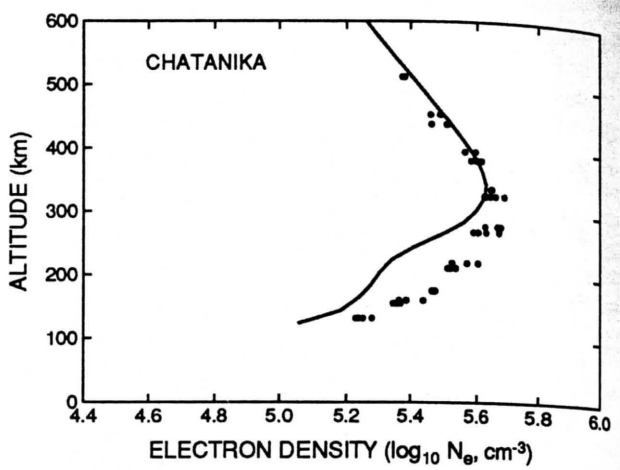

Fig. 7. Comparison of electron density measurements at 1200 MLT with model predictions. Chatanika measurements at 65° (± 1°) dipole latitude are plotted as solid circles and the solid line represents the corresponding ionospheric model results.

Figure 6. The solid line most closely matches the data in Figure 5 and represents a volume heating rate of 2.6 times standard and a heat flux of -0.7×10^{10} eV cm^{-2} s^{-1} at the upper boundary. Shown together with this reference curve are two sets of curves on either side. The lower temperature set corresponds to a heating rate of 2.0 times standard, and the higher temperature set corresponds to 3.0 times standard. The lower of each of the two sets of curves represents a heat flux of -0.4×10^{10} eV cm^{-2} s^{-1} and the upper of each of the two sets of curves represents a heat flux of -1×10^{10} eV cm^{-2} s^{-1}. A temperature difference of over 500° K is predicted at 600 km between the lowest curve (a heat flux of -0.4×10^{10} eV cm^{-2} s^{-1} and 2.0 times standard volume heating rate) and the highest curve (a heat flux of -1×10^{10} eV cm^{-2} s^{-1} and 3.0 times standard volume heating rate).

The rather clear indication from Figure 5 is that an increased volume heating rate is necessary to predict the temperature measurements of Millstone Hill. We now consider if an increased volume heating rate is also indicated by the Chatanika measurements. Figure 7 shows a comparison of the modeled profile of electron density and the Chatanika measurements (65° dipole latitude and 1200 MLT). The modeled results are accurate above 300 km, but they appreciably underestimate the electron density below the F_2 peak. Since the densities are underestimated below 300 km, it is possible that the dynamics of the F_2 peak were incorrectly modeled at this particular time and location. In particular, the electron density near the F_2 peak is sensitive to plasma drift along the magnetic field line, induced by the combined effects of ambipolar diffusion and neutral wind drag. *Sica et al.* [1988] have found this drift to rarely exceed 30–40 m/s, and it is unlikely that any errors in modeling field-aligned drifts of this magnitude would 'directly' affect electron temperatures. However, underestimating the electron density can have an effect on the electron temperature, as is seen in Figure 8, where model results are compared with Chatanika measurements. The solid line represents the electron temperature with the model densities, and the curve to the left of the solid line represents the predicted temperatures when the measured densities are substituted for the modeled ones (both of the two lower curves assume zero heat flux and a standard volume heating rate). The increase in ion density below the F_2 peak leads to increased cooling of the electrons and causes a 100°–200° decrease in electron temperature, centered about the region where the densities differ.

The two higher-temperature curves in Figure 8 represent an increase in the volume heating rate. The lower of the two curves is for an increase of 1.8 times standard, and the higher represents an increase of 2.6 times standard. The Chatanika data most nearly match the curve with a 1.8 times increase in the electron heating rate, while as shown in Figure 5, an increase of 2.6 times standard was needed for the Millstone Hill data.

Why is there a difference between the volume heating rates needed to fit the measurements of the two radars? There is a

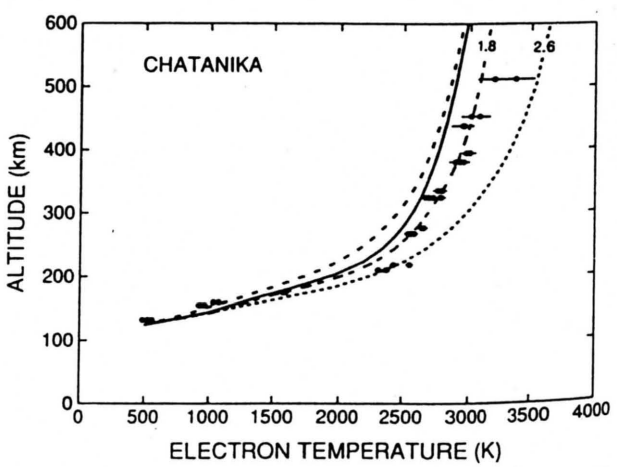

Fig. 8. A comparison of electron temperature measurements at 1200 MLT (± 0.5 hours) with model predictions assuming no heat flux at the upper boundary. Chatanika measurements at 65° (± 1°) dipole latitude are plotted as solid circles, and the curves represent the corresponding ionospheric model results. The solid line is for the standard volume heating rate. The dashed line to the left of the solid line is for the same conditions, but with the model electron densities adjusted to fit the measured densities. The dashed line immediately to the right of the solid line is for a factor of 1.8 increase in the volume heating rate, and the rightmost dashed line is for a factor of 2.6 increase in the volume heating rate.

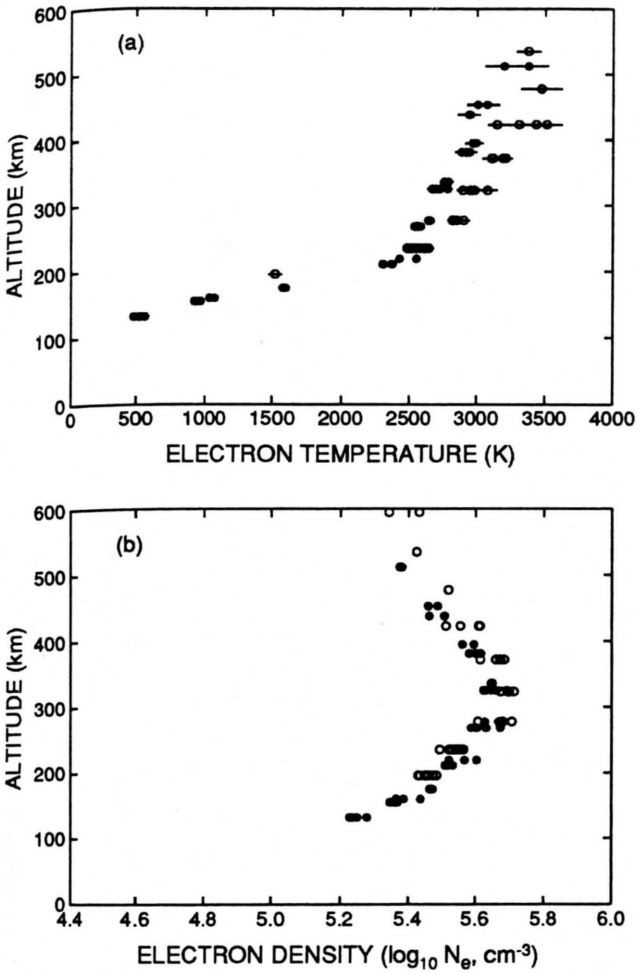

Fig. 9. A comparison of Chatanika and Millstone Hill (*a*) temperature measurements and (*b*) density measurements at 65° (±1°) and 1200 MLT (± 0.5 hours). The solid circles are Chatanika measurements, and the open circles are Millstone measurements.

difference in latitude between the two sets of radar measurements and a difference in the absolute time when the two sets of measurements were taken. There is also a difference in the solar zenith angle at 1200 MLT (see Figure 3*a*), but this is taken into account in the model. These differences could have an effect on the measurements, although even when the latitudinal difference is eliminated, there remains a difference between the two radar sites, as can be seen in Figure 9*a*, where the solid circles represent measurements at Chatanika and the open circles represent measurements at Millstone Hill. Both sets of measurements shown in Figure 9*a* were taken at 65° dipole latitude and at 1200 MLT. There is roughly a 200° difference in electron temperature measurements at high altitudes, with Millstone Hill measuring the highest temperatures.

Since the electron temperature depends sensitively upon the electron density, the Chatanika and Millstone Hill electron density measurements are plotted in Figure 9*b*. The conditions for these measurements are the same as for the electron temperature measurements plotted in Figure 9*a*. The density measurements agree quite well and probably cannot account for the temperature differences, especially since Millstone Hill density measurements are higher above the F_2 peak, which should correspond to lower temperatures.

A comparison is made between the diurnal variations of electron temperature and density for the two radar sites in Figures 10*a* and 10*b*, respectively. The solid circles correspond to Chatanika measurements and the open circles correspond to Millstone Hill measurements, both at 65° dipole latitude and 325 km. Throughout most of the daylight hours, Millstone Hill measured higher temperatures in accord with the results shown in Figure 9. However, in the early morning hours the differences can possibly be attributable to differences in density. Between 0500 and 0800 MLT, Millstone Hill measured lower densities, and therefore it is expected that the temperature measurements would be higher. In general, it appears that Millstone Hill measured a 200°–300° higher electron temperature than did Chatanika, not only at 1200 MLT but throughout most of the daylight hours. There are no apparent discrepancies (either instrumental or in data analysis) between Chatanika and Millstone Hill which can account for this temperature difference. It is important to note that, as mentioned above, the two sets of measurements are separated in geographic location and in universal time. However, since differences in solar EUV flux between the two sets of measurements are taken into account by the model, the 200°–300° difference in electron temperature can

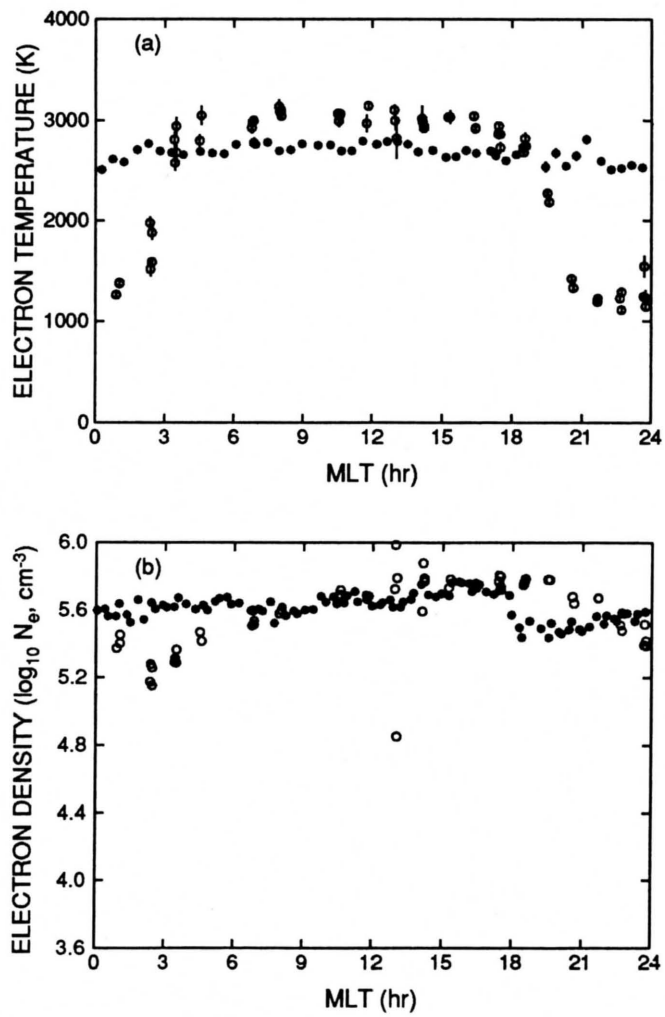

Fig. 10. A comparison of the diurnal variation in (*a*) temperature and (*b*) density measurements of the Chatanika and Millstone Hill radars at 65° (±1°) and 325 km altitude. The solid circles are Chatanika measurements, and the open circles are Millstone measurements.

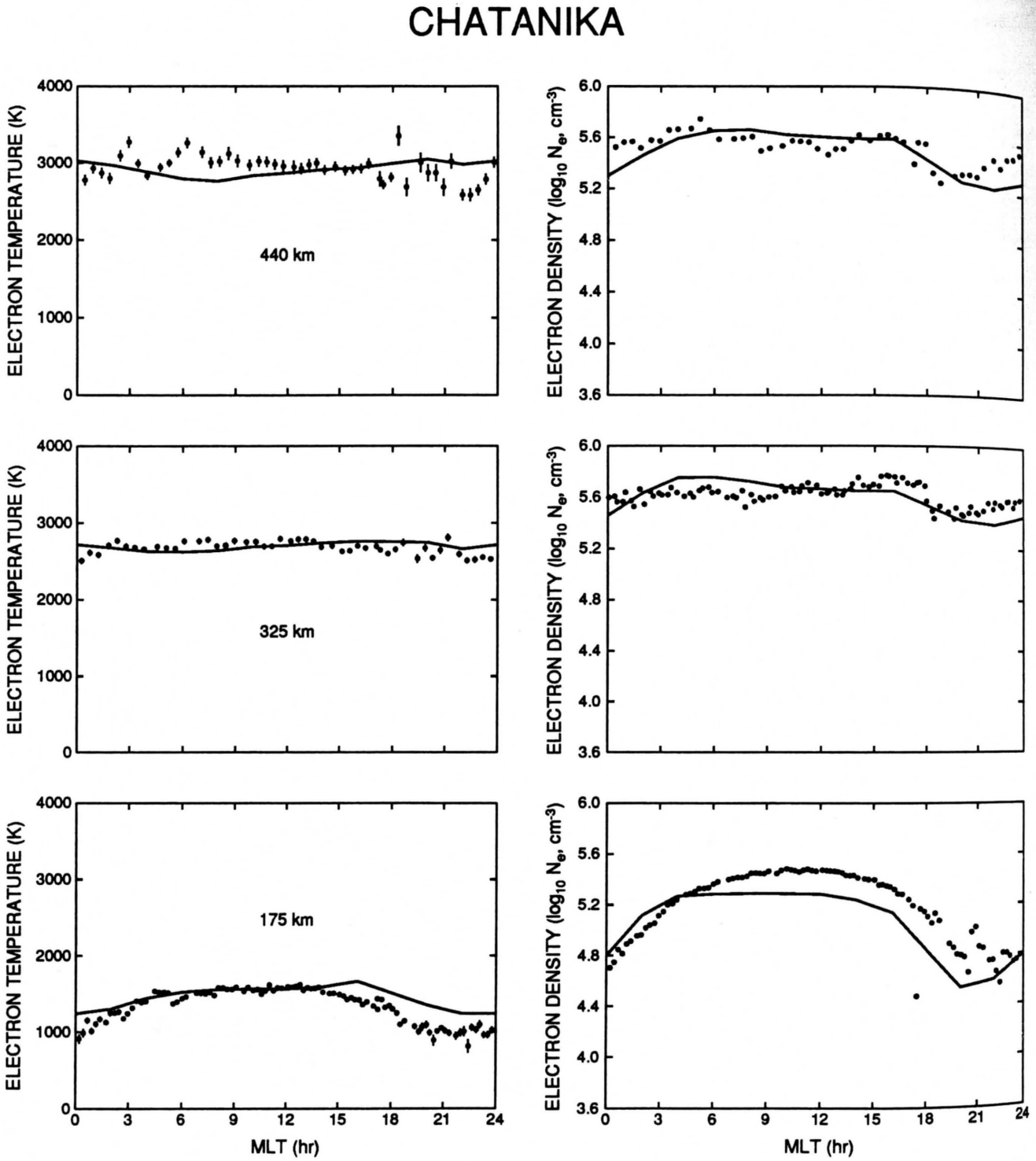

Fig. 11. Comparison of the model density and temperature predictions with Chatanika measurements at 65° (±1°) and at three different altitudes: 440 km (top panel); 325 km (middle panel); and 175 km (bottom panel). Electron temperatures are compared in the left column, and electron densities in the right. The model results are plotted as a solid line, and the radar measurements are plotted as solid circles.

only be explained in terms of modeling by differences in inputs, possibly either the volume heating rate or the heat flux at the upper boundary.

3.1. *Diurnal Variation*

In the next two figures, diurnal variations in the electron temperature predicted by the model are compared with measurements at Chatanika and Millstone Hill. In this comparison, differences in the volume heating rate and in the heat flux at the upper boundary are assumed between the two radar sites as discussed above. First, in Figure 11 we compare the ionospheric model results with the Chatanika measurements at three altitudes: 440 km (top panel); 325 km (middle panel); and 175 km (bottom panel). The temperature comparison is shown in the

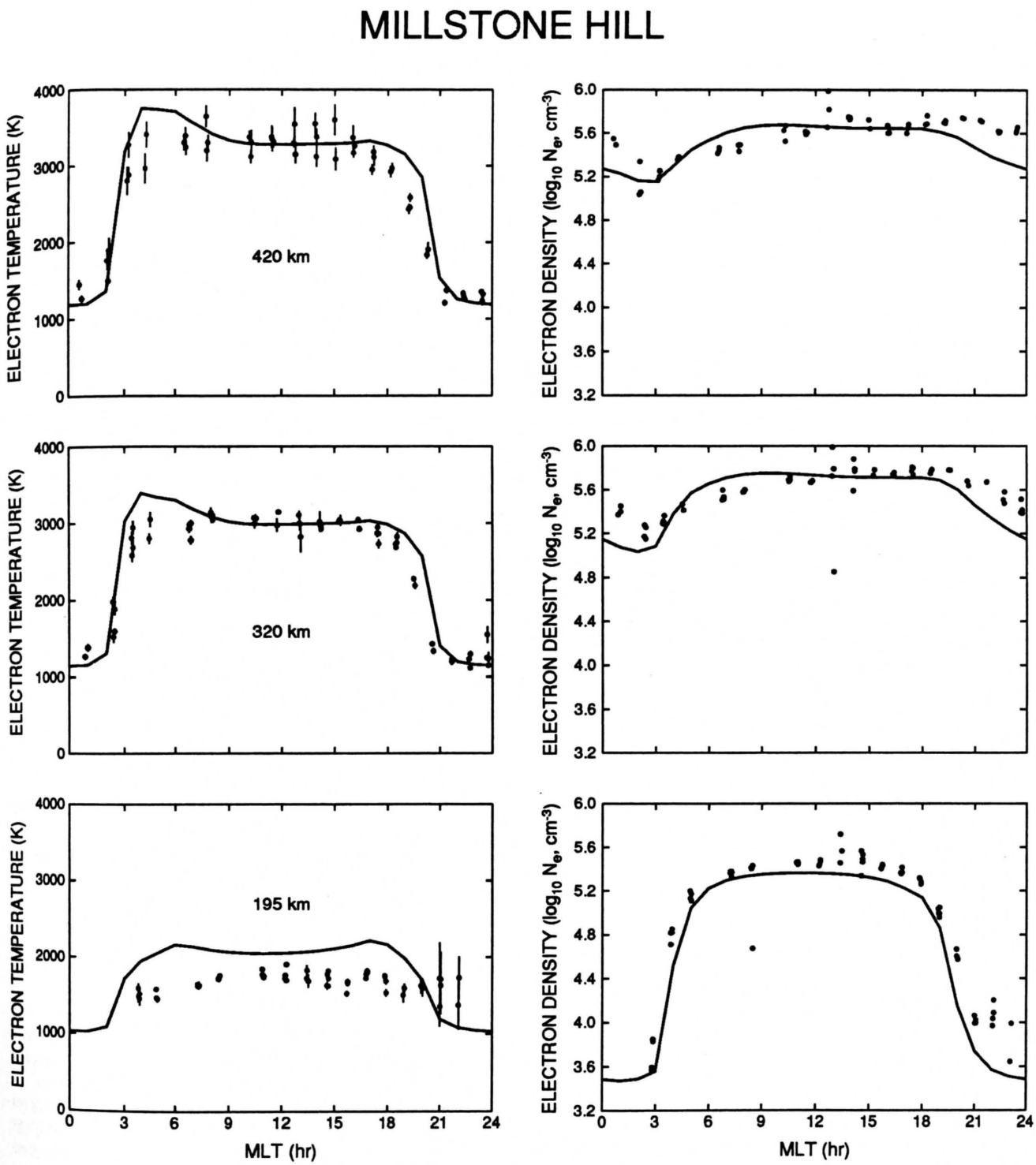

Fig. 12. Comparison of the model density and temperature predictions with Millstone Hill measurements at 55° (±1°) and at three different altitudes: 420 km (top panel); 320 km (middle panel); and 195 km (bottom panel). Electron temperatures are compared in the left column, and electron densities in the right. The model results are plotted as a solid line, and the radar measurements are plotted as solid circles.

left column and the density comparison in the right, all at 65° dipole latitude. The model temperatures are for a zero heat flux at the upper boundary and a factor of 1.8 increase in the volume heating rate. One of the most striking points about Figure 11 is that the temperature varies little during the course of a day, even though the zenith angle varies from 45° to 90°, as shown in Figure 3*a*. The model predicts quite well the diurnal variation in electron temperature, although in general, there seems to be a slight underestimate in the morning and a slight overestimate in the evening. These differences could be due to the slight overestimate of electron density in the morning and an underestimate in the evening, as shown in the right column.

In Figure 12 we compare the ionospheric model results with the Millstone Hill measurements at three altitudes: 420 km (top

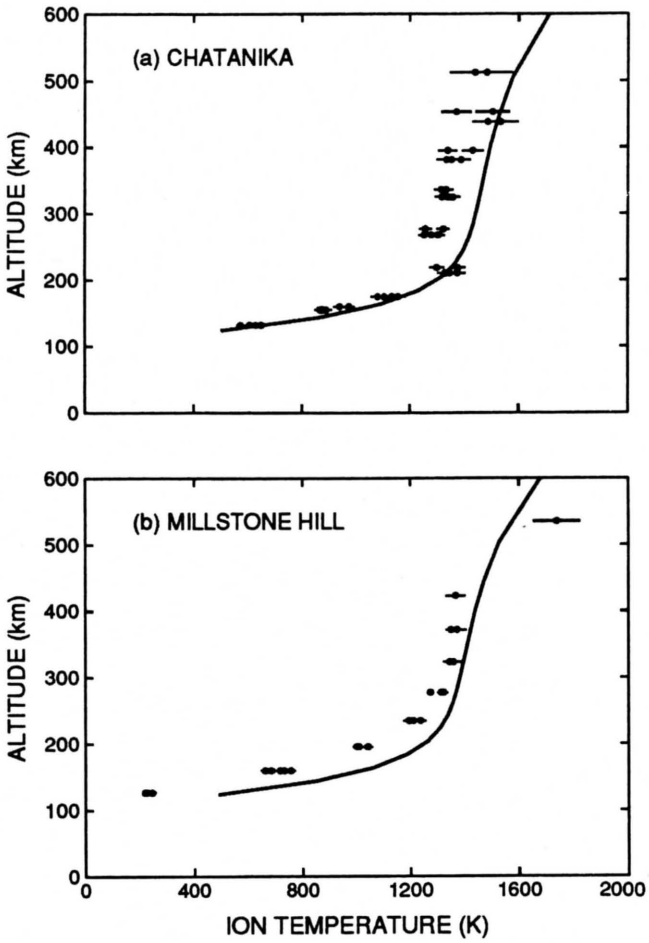

Fig. 13. Comparison of ion temperature measurements at 1200 MLT (± 0.5 hours) with model predictions. (*a*) Chatanika measurements at 65° (±1°) dipole latitude and (*b*) Millstone Hill measurements at 55° (±1°) dipole latitude, plotted as solid circles. The curves represent the corresponding ionospheric model results.

panel); 320 km (middle panel); and 195 km (bottom panel). The temperature comparison is shown in the left column and the density comparison in the right, all at 55° dipole latitude. The model temperatures are for a heat flux of -0.7×10^{10} eV cm^{-2} s^{-1} at the upper boundary and a factor of 2.6 increase in the volume heating rate. At this latitude, Millstone Hill is measuring a region that is in darkness during a portion of the evening hours. Thus, there is a strong MLT dependence, as opposed to the Chatanika measurements shown in Figure 11. In general, there is good agreement in the predicted and measured diurnal variation of the electron temperature, except for the overshoot in the predictions as the ionosphere enters sunlight after 0300 MLT. This overshoot does not seem to be caused by an underestimate in density, since the densities, if anything, are overestimated (at least between 0600 and 0900 MLT).

3.2. *Ion Temperature Comparisons*

We now compare ion temperature measurements with the results of the ionospheric model. First, however, specific terms in the equation for ion energy balance are discussed. An important source of energy for the ions is frictional heating due to **E** x **B** convection. The plasma convection pattern used in this study to model ion temperatures has been compared previously with measurements of ion convection from Chatanika and Millstone Hill and is not repeated here [see *Rasmussen et al.*, 1986]. The ions can also be heated (or cooled) via heat exchange with electrons and the neutral atmosphere. Thus, it is important, when modeling the ion temperature, to have an accurate estimate of the electron and, especially, the neutral temperature. We obtained an estimate of the neutral temperature from the MSIS model [*Hedin et al.*, 1977*a*, *b*], and the electron temperature used in the ion temperature comparisons is consistent with the results shown in Figures 11 and 12.

A comparison of the ion temperature measurements with the model at 1200 MLT is shown for Chatanika (65° dipole latitude) in Figure 13*a* and for Millstone Hill (55° dipole latitude) in Figure 13*b*. As can be seen in the figure, the model tends to overestimate the ion temperatures slightly for both Chatanika and Millstone Hill, although the predicted shape of the profile is quite good. We have also compared ion temperatures at other latitudes and times and have found, in general, good agreement with the measurements. Thus, it appears that, unlike the electron energy balance, the ion energy balance is well understood. Since a thorough parameter study of ion temperature behavior in the daytime high-latitude ionosphere has been conducted by *Schunk and Sojka* [1982], additional comparisons of ion temperature are not shown.

4. DISCUSSION

One of the major questions that is raised by this study is the increase in the volume heating rate that is seemingly required to predict the electron temperature measurements. Both radar measurements agree quite well with no heat flux at the top boundary and an increased volume heating rate, although the Millstone Hill measurements required a greater increase (2.6) in the heating rate than did those of Chatanika (1.8).

Recently, *Richards* [1986] has found that electron quenching of N(^2D) is a significant source of heat for ionospheric electrons. At solar maximum, this extra heating increases the heating rate at 250 km by a factor of 2. At solar minimum the increase is even more (a factor of 3.3). The magnitude of this additional heating term is very close to that found necessary to fit the measurements, which were taken at conditions near solar maximum. Since this extra heat source has not been included in our calculations, electron quenching of N(^2D) could explain the necessity to increase the volume heating rate in our results.

However, the electron temperature depends sensitively upon several parameters, including the electron density, the heat flux at the upper boundary, and the volume heating rate. Also, there are uncertainties in the cooling rates for ionospheric electrons, for example, in atomic oxygen fine structure cooling and in molecular nitrogen vibrational cooling. In addition, the electron temperature measurements require a knowledge of the average ion mass as a function of altitude, which is itself unknown and must be modeled. In light of these uncertainties, is one justified in singling out the volume heating rate as the parameter which is in error? Possibly not, as shown in Figure 14, where a comparison of model electron temperatures and measurements at Chatanika is made. The data are the same as shown in Figure 2. In Figure 14 the open circles represent electron temperature measurements assuming an ion transition altitude of 180 km and the solid circles a transition altitude of 225 km. The solid line represents the results of the model assuming electron densities measured at Chatanika and a heat flux of -2×10^{10} eV cm^{-2} s^{-1} at the upper boundary. In this instance, the volume heating rate has not been increased, and it is easy to see that with a

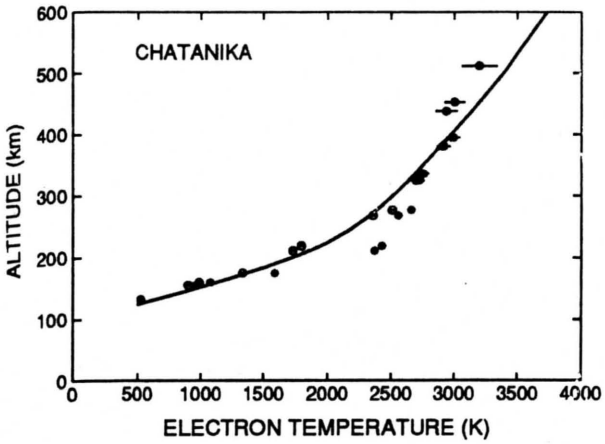

Fig. 14. Comparison of electron temperature measurements with model predictions. The open circles are Chatanika measurements assuming an ion transition altitude of 180 km and the solid circles are Chatanika measurements assuming an ion transition altitude of 225 km; both sets of measurements were taken at 65° (±1°) dipole latitude and 1200 MLT (± 0.5 hours). The solid line represents model predictions assuming no additional volume heating and a heat flux of -2×10^{10} eV cm^{-2} s^{-1} at the upper boundary.

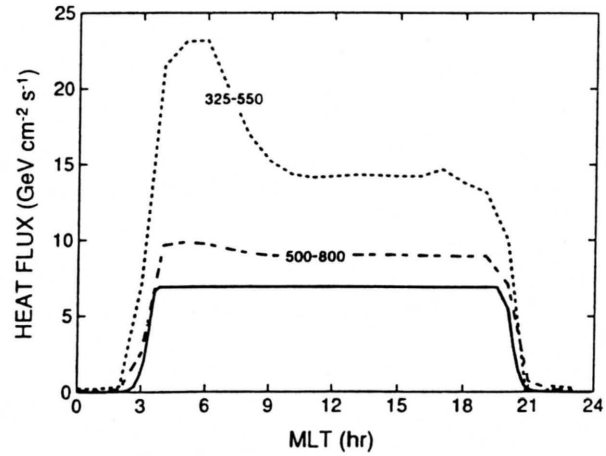

Fig. 15. Predictions of the magnitude of heat flux at the upper boundary as a function of MLT. The solid line represents input values to the model. The short-dashed line represents values obtained from equation (1) in the altitude range 325–550 km, and the long-dashed line in the altitude range 500–800 km.

somewhat different estimate for the transition height, thus changing the measurements to lie between the two extremes shown, the model predictions would agree very nicely with the measurements.

Because the heat flux at the upper boundary is such an important parameter in modeling the electron temperature, we examine the possibility of inferring this parameter from temperature measurements. At altitudes above the F region peak, thermal conduction dominates the electron energy balance, and one can obtain an approximate expression for the heat flux q_{et} at the upper boundary as a function of altitude z and electron temperature T_e,

$$q_{et} = -2.2 \times 10^5 \frac{(T_e^{7/2} - T_{eb}^{7/2})}{(z - z_b)} \quad (1)$$

where T_{eb} is the temperature at some reference altitude z_b [*Schunk*, 1983]. From equation (1), one can in principle find a value for q_{et} (in a least squares sense) from electron temperature data at high altitudes.

We have examined the uncertainties associated with equation (1) by applying it to our 'modeled' electron temperatures and seeing if the resulting value for the heat flux agrees with the input value for q_{et}. The results are shown in Figure 15, where the magnitude of the heat flux at the upper boundary is plotted as a function of MLT. The solid curve is the input value that was used in the model run, and the other two curves represent the inferred heat flux found by applying (1) to modeled temperatures in two different altitude ranges (325–550 km and 500–800 km). When the lower altitude range is used (short-dashed curve), the heat flux determined from (1) is overestimated by a factor of 3 to 4 because other terms in the electron energy balance are important besides thermal conduction. At altitudes above 500 km, a better estimate for q_{et} is obtained from (1), as shown by the long-dashed line. Because of limited radar data above 500 km, we were unable to obtain reliable estimates of q_{et} from equation (1) for this study.

The various uncertainties involved in modeling the electron temperature, as well as in the reduction of the data, make it difficult to unequivocally determine what is physically taking place. In regard to this, we conclude by summarizing the effects of some of the uncertainties present in this study. Differences between the modeled electron density and measurements were shown to have a 100°–200° effect on the modeled electron temperature. Uncertainty in the mean ion mass can lead to a 600°–700° difference in the inferred electron temperature near 200 km, while a 400° difference at 300 km was noted due to uncertainties in the volume heating rate. The heat flux at the upper boundary is even more important, as a 1000° difference was noted at 600 km for a reasonable range of the magnetospheric heat flux.

Acknowledgments. We thank the many SRI and MIT Haystack personnel who have helped make this research possible. In particular, we appreciate the considerable efforts of Carol Leger. The SRI portion of this research was supported by AFOSR contracts F49620-83-K-0005 and F49620-87-K-0007, the Utah State University portion by AFOSR contract F49620-86-C-0109 and NOAA contract ATM81-19477, and the Millstone Hill portion by AFOSR-86-0023B.

The Editor thanks D. Alcayde and R. J. Moffett for their assistance in evaluating this paper.

REFERENCES

Baron, M. J., The Chatanika Radar System, in *Radar Probing of the Auroral Plasma,* edited by A. Brekke, pp. 103–141, Universitetsforlaget, Tromso, Norway, 1977.

Conrad, J. R., and R. W. Schunk, Diffusion and heat flow equations with allowance for large temperature differences between interacting species, *J. Geophys. Res., 84,* 811–822, 1979.

de la Beaujardiere, O., V. B. Wickwar, M. J. Baron, J. Holt, R. M. Wand, W. L. Oliver, P. Bauer, M. Blanc, C. Senior, D. Alcayde, G. Caudal, J. Foster, E. Nielsen, and R. Heelis, MITHRAS: A brief description, *Radio Sci., 19,* 665–673, 1984.

Foster, J. C., J. R. Doupnik, and G. S. Stiles, Large scale patterns of auroral ionospheric convection observed with the Chatanika radar, *J. Geophys. Res., 86,* 11357–11371, 1981.

Hedin, A. E., J. E. Salah, J. V. Evans, C. A. Reber, G. P. Newton, N. W. Spencer, D. C. Kayser, D. Alcayde, P. Bauer, L. Cogger, and J. P. McClure, A global thermospheric model based on mass spectrometer and incoherent scatter data MSIS, 1, N_2 density and temperature, *J. Geophys. Res., 82,* 2139–2147, 1977*a*.

Hedin, A. E., C. A. Reber, G. P. Newton, N. W. Spencer, H. C. Brinton, H. G. Mayr, and W. E. Potter, A global thermospheric model based on mass spectrometer and incoherent scatter data MSIS, 2, Composition, *J. Geophys. Res., 82, 2148–*2156, 1977*b*.

Kofman, W., and V. B. Wickwar, Plasma line measurements at Chata-

nika with high-speed correlator and filter bank, *J. Geophys. Res., 85*, 2998–3012, 1980.

Lathuillere, C., and A. Brekke, Ion compositions in the auroral ionosphere as observed by EISCAT, *Ann. Geophys., 3*, 557–568, 1985.

Lathuillere, C., G. Lejeune, and W. Kofman, Direct measurements of ion composition with EISCAT in the high latitude *F*1 region, *Radio Sci., 18*, 887–893, 1983.

Rasmussen, C. E., R. W. Schunk, J. J. Sojka, V. B. Wickwar, O. de la Beaujardiere, J. Foster, J. Holt, D. S. Evans, and E. Nielsen, Comparison of simultaneous Chatanika and Millstone Hill observations with ionospheric model predictions, *J. Geophys. Res., 91*, 6986–6998, 1986.

Richards, P. G., Thermal electron quenching of N(^2D): Consequences for the ionospheric photoelectron flux and the thermal electron temperature, *Planet. Space Sci., 34*, 689–694, 1986.

Schunk, R. W., The terrestrial ionosphere, in *Solar-Terrestrial Physics*, edited by R. L. Carovillano and J. M. Forbes, pp. 609–676, D. Reidel, Hingham, Mass., 1983.

Schunk, R. W., and A. F. Nagy, Electron temperatures in the *F* region of the ionosphere: Theory and observations, *Rev. Geophys., 16*, 355–399, 1978.

Schunk, R. W., and W. J. Raitt, Atomic nitrogen and oxygen ions in the daytime high-latitude *F* region, *J. Geophys. Res., 85*, 1255–1272, 1980.

Schunk, R. W., and J. J. Sojka, Ion temperature variations in the daytime high-latitude *F* region, *J. Geophys. Res., 87*, 5169–5183, 1982.

Schunk, R. W., and J. C. G. Walker, Transport properties of the ionospheric electron gas, *Planet. Space Sci., 18*, 1535–1550, 1970.

Schunk, R. W., and J. C. G. Walker, Theoretical ion densities in the lower ionosphere, *Planet. Space Sci., 21*, 1875–1896, 1973.

Schunk, R. W., W. J. Raitt, and P. M. Banks, Effect of electric fields on the daytime high-latitude *E* and *F* regions, *J. Geophys. Res., 80*, 3121–3130, 1975.

Schunk, R. W., P. M. Banks, and W. J. Raitt, Effects of electric fields and other processes upon the nighttime high latitude *F* layer, *J. Geophys. Res., 81*, 3271–3282, 1976.

Schunk, R. W., J. J. Sojka, and M. D. Bowline, Theoretical study of the electron temperature in the high latitude ionosphere for solar maximum and winter conditions, *J. Geophys. Res., 91*, 12,041–12,054, 1986.

Sica, R. J., R. W. Schunk, and C. E. Rasmussen, Can the high latitude ionosphere support large field-aligned ion drifts?, *J. Atmos. Terr. Phys.*, in press, 1988.

Sojka, J. J., and R. W. Schunk, A theoretical study of the global *F* region for June solstice, solar maximum, and low magnetic activity, *J. Geophys. Res., 90*, 5285–5298, 1985.

Sojka, J. J., W. J. Raitt, and R. W. Schunk, Effect of displaced geomagnetic and geographic poles on high-latitude plasma convection and ionospheric depletions, *J. Geophys. Res., 84*, 5943–5951, 1979.

Sojka, J. J., W. J. Raitt, and R. W. Schunk, A theoretical study of the high-latitude winter *F* region at solar minimum for low magnetic activity, *J. Geophys. Res., 86*, 609–621, 1981*a*.

Sojka, J. J., W. J. Raitt, and R. W. Schunk, Theoretical predictions for ion composition in the high-latitude winter *F* region for solar minimum and low magnetic activity, *J. Geophys. Res., 86*, 2206–2216, 1981*b*.

Sojka, J. J., R. W. Schunk, J. V. Evans, J. M. Holt, and R. H. Wand, Comparison of model high-latitude electron densities with Millstone Hill observations, *J. Geophys. Res., 88*, 7783–7793, 1983.

Sterling, D. L., W. B. Hanson, R. J. Moffett, and R. G. Baxter, Influence of electromagnetic drifts and neutral air winds on some features of the F_2 region, *Radio Sci., 4*, 1005–1023, 1969.

O. de la Beaujardiere and V. B. Wickwar, SRI International, 333 Ravenswood Ave., Menlo Park, CA 94025.

J. Foster and J. Holt, MIT Haystack Observatory, Westford, MA 01886.

C. E. Rasmussen, R. W. Schunk, and J. J. Sojka, Center for Atmospheric and Space Sciences, Utah State University, UMC 4405, Logan, UT 84322.

(Received June 26, 1987;
revised October 7, 1987;
accepted October 29, 1987.)